BIOCHEMISTRY
including biophysical chemistry & molecular biology

Article

pubs.acs.org/biochemistry

Two Divalent Metal Ions and Conformational Changes Play Roles in the Hammerhead Ribozyme Cleavage Reaction

Aamir Mir,[‡,#] Ji Chen,[‡,#] Kyle Robinson,[‡] Emma Lendy,[‡] Jaclyn Goodman,[‡] David Neau,[§] and Barbara L. Golden*[,‡]

[‡]Department of Biochemistry, Purdue University, West Lafayette, Indiana 47907, United States

[§]Department of Chemistry and Chemical Biology, Cornell University, Northeastern Collaborative Access Team, Argonne National Laboratory, Argonne, Illinois 60439, United States

Supporting Information

ABSTRACT: The hammerhead ribozyme is a self-cleaving RNA broadly dispersed across all kingdoms of life. Although it was the first of the small, nucleolytic ribozymes discovered, the mechanism by which it catalyzes its reaction remains elusive. The nucleobase of G12 is well positioned to be a general base, but it is unclear if or how this guanine base becomes activated for proton transfer. Metal ions have been implicated in the chemical mechanism, but no interactions between divalent metal ions and the cleavage site have been observed crystallographically. To better understand how this ribozyme functions, we have solved crystal structures of wild-type and G12A mutant ribozymes. We observe a pH-dependent conformational change centered around G12, consistent with this nucleotide becoming deprotonated. Crystallographic and kinetic analysis of the G12A mutant reveals a Zn^{2+} specificity switch suggesting a direct interaction between a divalent metal ion and the purine at position 12. The metal ion specificity switch and the pH−rate profile of the G12A mutant suggest that the minor imino tautomer of A12 serves as the general base in the mutant ribozyme. We propose a model in which the hammerhead ribozyme rearranges prior to the cleavage reaction, positioning two divalent metal ions in the process. The first metal ion, positioned near G12, becomes directly coordinated to the O6 keto oxygen, to lower the pK_a of the general base and organize the active site. The second metal ion, positioned near G10.1, bridges the N7 of G10.1 and the scissile phosphate and may participate directly in the cleavage reaction.

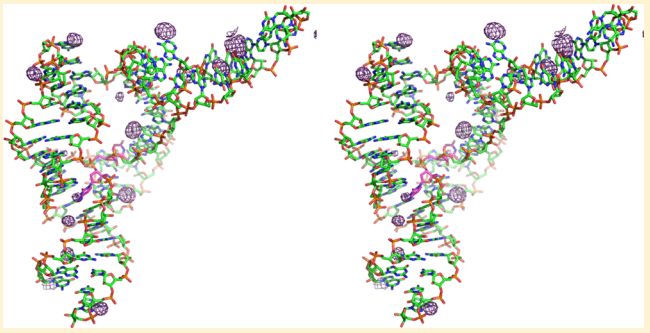

In 1987, Olke Uhlenbeck first reported the existence of a small, self-cleaving RNA known as the hammerhead ribozyme.[1] This compact RNA catalyst was composed of three short base-paired stems and a cluster of core nucleotides. Although these minimal hammerhead ribozymes are functional, it was eventually discovered that maximal activity requires some form of tertiary interaction between stems I and II (Figure 1A). Using the known conserved elements of the hammerhead ribozyme, several groups have used bioinformatics and secondary structure predictions to search for hammerhead-like sequences in the available genomes. Now, thousands of hammerhead ribozyme sequences have been identified in a variety of species, spanning all domains of life.[2−5] While many viroids use hammerhead ribozyme sequences to process their RNA genomes, the physiological functions of the majority of these hammerhead-like sequences are still unclear.

Although the hammerhead ribozyme was the first small nucleolytic ribozyme to be discovered, its catalytic mechanism remains elusive. Most small nucleolytic ribozymes often cleave their target RNAs by activating a 2′-hydroxyl for nucleophilic attack at the phosphate of the adjacent nucleotide (Figure 2). The 5′-hydroxyl of the following nucleotide is released, generating 2′,3′-cyclic phosphate and 5′-hydroxyl termini on the products. This reaction requires deprotonation of the 2′-hydroxyl that serves as the nucleophile and protonation of the 5′-hydroxyl leaving group. The mechanism by which this reaction occurs, however, varies from ribozyme to ribozyme.

Small nucleolytic ribozymes can be divided into two distinct classes based on their ability to react in the presence of $[Co(NH_3)_6]^{3+}$.[6] $[Co(NH_3)_6]^{3+}$ is a trivalent ion with nonexchangable ligands that mimics hydrated Mg^{2+} ions. Unlike $[Mg(H_2O)_6]^{2+}$, $[Co(NH_3)_6]^{3+}$ cannot coordinate directly to ligands from the RNA, and $[Co(NH_3)_6]^{3+}$ does not readily participate in proton transfer reactions because the pK_a of the amine ligands of $[Co(NH_3)_6]^{3+}$ is much higher than that of a Mg^{2+}-bound water.[7] Class I ribozymes, such as the hairpin ribozyme, glmS ribozyme, and twister ribozyme can react in the presence of $[Co(NH_3)_6]^{3+}$ alone.[8−12] Consistent with this lack of dependence on Mg^{2+}, none of these ribozymes appear to use metal ion-mediated catalysis in the reaction

Received: July 22, 2015
Revised: September 23, 2015
Published: September 23, 2015

DOI: 10.1021/acs.biochem.5b00824
Biochemistry 2015, 54, 6369−6381

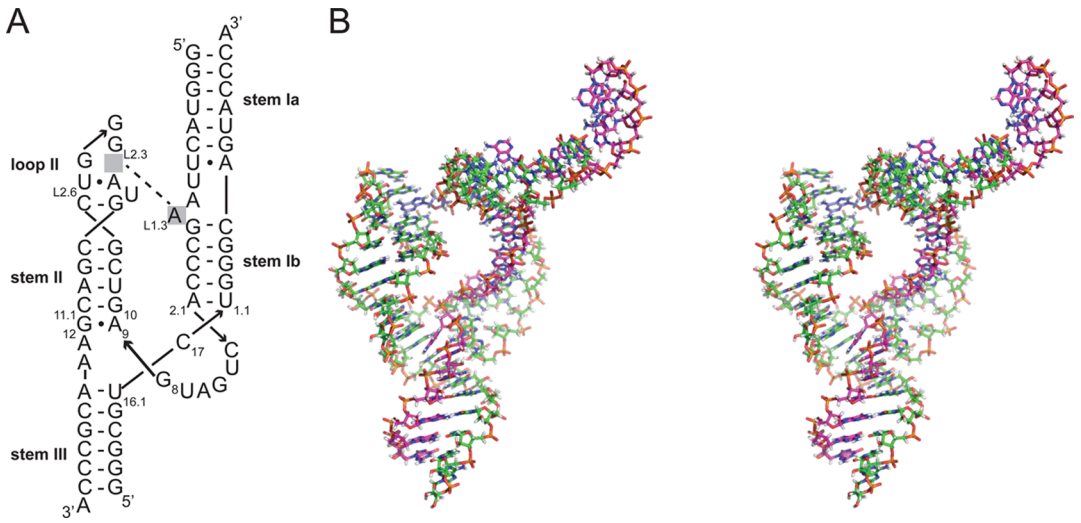

Figure 1. Secondary structure and tertiary structure of the hammerhead ribozyme. (A) The RzB hammerhead ribozyme folds into three helical domains, stem I, stem II, and stem III. Stem I is interrupted by an internal loop, and stem II is capped by loop II. A single adenosine base, A(L1.3), from stem I makes a tertiary contact within loop II. The numbering system used here was described by Hertel et al.[66] (B) The tertiary structure of the RzB ribozyme (wall-eyed stereo).

mechanism. Class I ribozymes use nucleobase or cofactors to perform general acid or general base catalysis. In many class I ribozymes, the pK_a of the general acid is shifted by the active site environment toward neutrality, increasing the population of the catalytically active protonation state.[13−16]

In contrast, class II ribozymes, such as the hammerhead and hepatitis delta virus (HDV) ribozymes, do not have high activity in the presence of $[Co(NH_3)_6]^{3+}$ alone, and their Mg^{2+}-dependent reaction is strongly inhibited by the presence of $[Co(NH_3)_6]^{3+}$.[17−19] Recent crystallographic studies have demonstrated that the hepatitis delta virus ribozyme binds a Mg^{2+} ion within its active site.[20] Mutational analyses and simulations suggest that this Mg^{2+} ion participates in the cleavage reaction.[21,22] On the basis of the response of the hammerhead ribozyme to $[Co(NH_3)_6]^{3+}$, this ribozyme would also be predicted to use Mg^{2+} ions in its catalytic mechanism.[18]

A Mg^{2+}-independent mechanism for the hammerhead ribozyme has been proposed based on cross-linking studies, kinetic analyses, and the crystal structure of the *Schistosoma mansoni* hammerhead ribozyme.[23−26] In this mechanism, the nucleobase of G12 serves as a general base to abstract the proton from the 2′-hydroxyl that serves as the nucleophile. The N1 of G12 would therefore need to be deprotonated, and negatively charged, prior to cleavage (Figure 1). The general acid was proposed to be 2′-hydroxyl of G8 which is observed to be hydrogen bonded to the 5′-hydoxyl leaving group in crystal structures.

This proposed mechanism is problematic for several reasons. The pK_a's of N1 of G12 and 2′-OH of G8 are ∼9 and ∼13 respectively if they are not shifted by the active site environment. These pK_a values are far from neutrality, and, unless their pK_a's are shifted by the active site, are not optimized for general acid−base catalysis near neutrality as the fraction of ribozyme in the active state would be very small.[27] It is not clear what elements within the hammerhead ribozyme would serve to shift the pK_a's of the proposed general acid and general base.

There is also considerable evidence from solution biochemical experiments that a divalent metal ion, such as Mg^{2+}, is involved in the cleavage reaction. A direct interaction between a metal ion and the pro-R_P oxygen of the scissile phosphate has been proposed based on metal rescue of phosphorothioate-substituted substrates.[28−31] While the hammerhead ribozyme is capable of reaction in the absence of divalent metal ions,[32] very high concentrations of monovalent ions are required to promote cleavage under these conditions, and the reaction appears to proceed though an alternate channel.[18,29]

Divalent metals have been shown to produce considerable rate enhancements when compared to reactions in their absence,[33] and the rate constant of the reaction appears to be affected by the identities of the divalent metals used.[34] For example, reactions in Mn^{2+} proceed faster than Zn^{2+} or Mg^{2+}. Crystal structures and electron paramagnetic resonance experiments have revealed a high affinity Mn^{2+} binding site at the A9−G10.1 region;[35−37] however based on crystal structures, this ion cannot interact directly with the cleavage site. York and colleagues have performed molecular dynamics simulations that suggest prior to catalysis a metal ion moves from the position near G10.1 observed in the crystal structure to the scissile phosphate where it is well-positioned to participate in catalysis.[38−40] Together, these studies point to significant roles for divalent metal ions in the cleavage reaction of the hammerhead ribozyme under cellular conditions.

To address these open questions in what may be the most heavily investigated of the known small nucleolytic ribozyme, we have reinvestigated the crystal structure of the hammerhead ribozyme using an artificial hammerhead ribozyme, RzB, generated by the Burke laboratory.[41] Compared to the *S. mansoni* and satellite tobacco ringspot virus hammerhead ribozymes previously studied,[24,26,42] this ribozyme has a different tertiary interaction between stems I and II, crystallizes under different conditions, and has distinctly different crystal packing interactions. In spite of these differences, the active site structure is not significantly different than the previously determined structures.

We therefore examined the activity, metal specificity, and the pH−rate profiles of ribozymes with various mutations. We found that the solution biochemical results were not fully consistent with the crystal structures. We identify two divalent

DOI: 10.1021/acs.biochem.5b00824
Biochemistry 2015, 54, 6369−6381

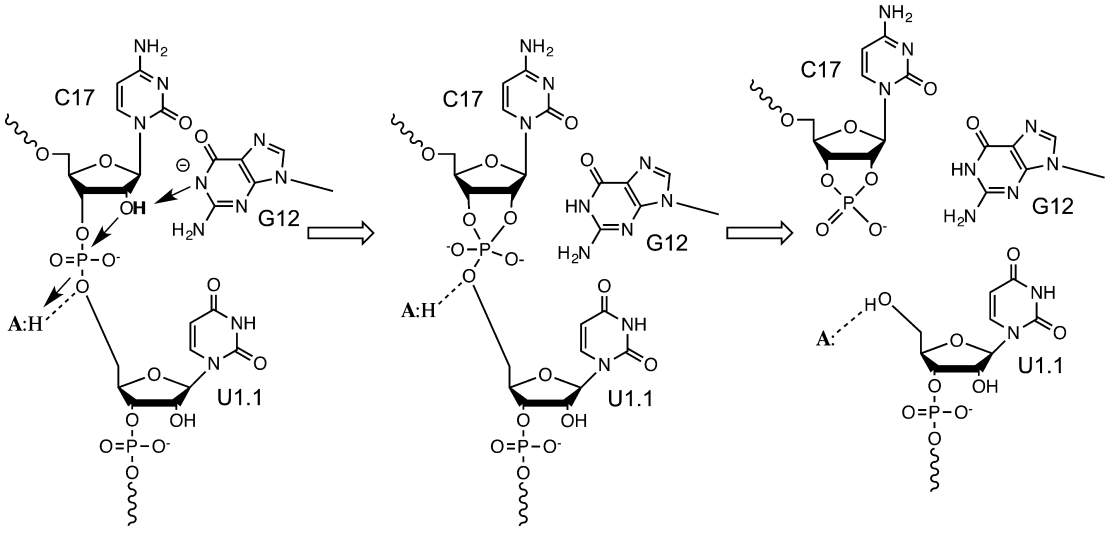

Figure 2. Cleavage reaction of the hammerhead ribozyme. Small nucleolytic ribozymes cleave their substrates by activating a 2′-O for attack at the phosphate of the following nucleotide and release of the 5′-OH. G12 appears to serve as a general base, accepting a proton from the 2′-OH of the nucleophile. A general acid (A:H) could facilitate catalysis by donating a proton to the 5′-O leaving group.

ion binding sites which have the potential to directly contribute to metal-mediated catalysis in the hammerhead ribozyme. Taken together, these data suggest that the ground state of the hammerhead ribozyme observed in crystal structures does not represent a catalytically active conformation, but rather a precatalytic state that must rearrange, at least subtly prior to catalysis.[31,38]

MATERIALS AND METHODS

RNA Synthesis. The two trans-acting versions of the hammerhead ribozyme were designed based on the previously reported sequences of the SELEX derived RzB[41] and the *S. mansoni* ribozyme.[24] To make the ribozyme strand, the ribozyme sequence was placed between a T7 promotor and an EarI restriction site, which was then inserted into pUC-19 and amplified in *Escherichia coli* DH5α cells. DNA plasmid was obtained using QIAGEN Mega kit. *In vitro* transcription and RNA purification by denaturing polyacrylamide gel electrophoresis (PAGE) were performed as previously described.[43] The RNA sample was concentrated using an Amicon Ultra centrifugal filter and stored at −20 °C.

For crystallization, a 20-nt inhibitor strand carrying a 2′-deoxy modification at the C17 position was purchased from Thermo Scientific, deprotected according to manufacturer's guidelines, and further purified by denaturing PAGE gel. For solution kinetic experiments, an all ribose substrate used was chemically synthesized and DY-547 labeled at its 5′-end.

RNA Crystallization. To refold the hammerhead ribozyme, equal molar concentrations of ribozyme strand and the inhibitor strand were mixed in a buffer containing 10 mM potassium cacodylate at pH 6.0. The complex was heated at 90 °C for 1 min and cooled to room temperature for 10 min. $MgCl_2$ was then added to the complex to achieve a concentration of 10 mM. Following addition of Mg^{2+}, the complex was heated at 50 °C for 5 min and cooled to room temperature for 20 min prior to use. The final concentration of the refolded complex was 5.5 mg/mL.

The ribozyme−inhibitor complex was crystallized by vapor diffusion using hanging drops. Drops were created by mixing 1 or 2 μL of the refolded complex with 1 μL of a reservoir solution containing 33% MPD, 0.4 M potassium chloride, 50 mM potassium acetate pH 5.0, and 0.5 mM spermine. The drops were equilibrated against 1 mL of reservoir solution in a Linbro plate (Hampton Research) at room temperature. Ribozyme crystals started to appear in ∼4 weeks and grew to the size of ∼0.2 mm × 0.1 mm × 0.05 mm in the next few weeks. Prior to data collection, crystals were soaked into a solution containing 33% MPD, 50 mM potassium acetate pH 5.0 or Tris-HCl pH 8.0, 5% isopropanol, 0.4 M potassium chloride, 1 mM spermine, and 50 mM $MgCl_2$ for 0.5−1 h. For anomalous diffraction experiments, crystals were soaked in buffers containing 10 mM $MnCl_2$ and 50 mM Tris·HCl pH 8.0, 50 mM $MnCl_2$ and potassium acetate pH 5.0 or 10 mM $Zn(O_2CCH_3)_2$ and 50 mM potassium acetate pH 5.0. In addition to the divalent metal ions and buffers, each solution contained 5% isopropanol, 33% MPD, 0.4 M potassium chloride, and 1 mM spermine. Crystals were then flash-frozen and stored in liquid nitrogen.

Diffraction data were collected at LS-CAT or NE-CAT beamlines at the Advanced Photon Source (Argonne National Laboratory, Argonne, IL). Data were processed by HKL2000[44] in space group $C222_1$.

Structure Determination and Refinement. The search model used for molecular replacement was derived from the crystal structure of *S. mansoni* hammerhead ribozyme (PDB code: 3ZD5). The entire stem I region, the stem II loop, and active site residues including C3, G8, A9, G12, C17, and C1.1 were removed from the search model. The phase was determined using Phaser in Phenix.[45] The asymmetric unit contains a single ribozyme and the best solution had a TFZ score of 8.8 and an LLG of 222. The initial model was improved by the Autobuild routine implemented in Phenix. The initial model was improved by several rounds of manual building and refinement using Coot[46] and Phenix. Waters and Mg^{2+} ions were manually modeled using Coot. Variants of the initial structure solution were refined using a constant set of test set of reflections used to calculate R_{free} in the initial structure.

Kinetic Assays. Single turnover reactions were performed under various conditions to obtain observed rate constants k_{obs}. Ribozyme (2 μM) was mixed with 50 nM fluorescently labeled

DOI: 10.1021/acs.biochem.5b00824
Biochemistry 2015, 54, 6369−6381

Table 1. Crystallographic Data Collection and Refinement Statistics

	WT RzB			G12A		
data collection	pH 5.0 Mg^{2+}	pH 5.0 Mn^{2+}	pH 8.0 Mn^{2+}	pH 5.0 Zn^{2+}	pH 4.0 Mn^{2+}	pH 5.0 Mg^{2+}
PDB id	5DQK	5DI4	5DI2	5DH8	5DH7	5DH6
cell dimensions *a*, *b*, *c* (Å)	79.76, 86.07, 103.3	80.40, 86.05, 104.21	79.52, 85.88, 103.72	80.94, 86.02, 103.37	81.3, 85.8, 103.5	81.41, 85.96, 102.97
wavelength (Å)	0.97872	1.5011	1.5011	1.181	1.8923	0.976
resolution (Å)	42.0−2.70 (2.75−2.70)	50.0−2.94 (2.99−2.94)	50.0−3.00 (3.05−3.00)	*50.0−3.10 (3.15−3.00)*	50.0−3.08 (3.13−3.08)	50.0−2.80 (2.85−2.80)
R_{merge} (%)	5.9 (78.5)	7.6 (37.9)	8.9 (33.7)	11.9 (28.6)	13.5 (25.2)	7.8 (65.5)
$I/\sigma(I)$	28 (2.5)	36.9 (7.7)	34.4 (14.1)	49.4 (22.4)	26.5 (6.0)	61.7 (6.3)
no. of reflections	9951	14606	13895	12541	12239	9318
redundancy	8.1 (8.3)	14.2 (14.5)	13.6 (14.6)	13.3 (14.6)	4.4 (3.0)	14.3 (15.0)
completeness (%)	99.7 (100)	99.8 (100.0)	99.8 (100.0)	99.5(95.6)	92.9 (70.2)	99.5 (96.7)
Refinement						
resolution (Å) (last shell)	26.1−2.71 (2.85−2.71)	28.2−2.95 (3.05−2.95)	39.8−2.99 (3.10−2.99)	28.3−3.30 (3.47−3.29)	40.0−3.06 (3.19−3.06)	28.4−2.78 (2.93−2.78)
no. of reflections	9627	14432	13759	10413	12124	9231
no. of reflections in the test set	968	1446	1385	1048	1206	920
R_{work}/R_{free} (%) (last shell)	22.42/27.78 (36.14/42.27)	20.94/23.30 (30.54/29.65)	22.10/25.99 (25.85/32.97)	21.68/25.18 (21.97/30.91)	20.20/25.37 (26.49/33.52)	21.08/24.16 (35.27/36.02)
no. of atoms	1479	1466	1462	1467	1465	1467
RNA	1455	1455	1455	1454	1454	1454
ions	5	11	7	13	11	5
water	19	0	0	0	0	8
average *B*-factor	27.1	76.30	73.37	74.40	86.62	56.1
root-mean-square deviation						
bond length (Å)	0.008	0.001	0.001	0.001	0.001	0.002
bond angles (deg)	1.378	0.388	0.373	0.443	0.376	0.470
coordinate error (Å)	0.45	0.32	0.38	0.33	0.34	0.37

DOI: 10.1021/acs.biochem.5b00824
Biochemistry 2015, 54, 6369−6381

substrate in 50 mM buffer adjusted to a desired pH. Buffers used were potassium acetate pH 4.5 or 5.0, MES pH 5.5, 6.0 or 6.5, MOPS pH 7.0, and Tris-HCl pH 7.5, 8, or 8.5. The mixture was then heated at 90 °C for 2 min, cooled to room temperature for 10 min, and equilibrated at 37 °C for 2 min. Reactions were initiated using 5 μL of initiation buffers which contained the appropriate divalent metal ion ($MgCl_2$, $MnCl_2$, or $Zn(O_2CCH_3)_2$) at the desired concentration and 50 mM buffer. At various time intervals, 5 μL aliquots of reaction were thoroughly mixed, on ice, with 5−20 μL of the quenching buffer (25 mM EDTA, 0.5× TBE, and 90% formamide) to ensure efficient quenching. The progress of the reaction was analyzed by separating the cleaved and uncleaved substrate on denaturing (7 M urea) 10% acrylamide gels, detecting the emission of DY-547 on Typhoon FLA9500 variable mode imager (GE Healthcare) and quantifying bands using ImageQuant 5.1 (GE Healthcare). Fraction cleaved (f) values were plotted against time (t) using KaleidaGraph (Synergy Software) and data were fit to a single exponential equation:

$$f = A + B[e^{(-k_{obs}t)}] \quad (1)$$

where A is the fraction cleaved at completion, $A + B$ is the burst fraction, and k_{obs} is the first order rate constant. For very slow reactions, A was artificially set at 0.9.

To find apparent pK_a values, k_{obs} values obtained from eq 1 were plotted as a function of pH, and the data were fit to a linear equation or eqs 2 or 3 as appropriate:

$$k_{obs} = k_{max}/[1 + 10^{(pK_a - pH)}] \quad (2)$$

$$k_{obs} = k_{max}/[1 + 10^{(pK_{a1} - pH)} + 10^{(pH - pK_{a2})} + 10^{(pK_{a1} - pK_{a2})}] \quad (3)$$

Metal titration experiments were fit to eq 4:

$$k_{obs} = k_{max}/[1 + (K_{D,M^{2+}}/[M^{2+}])^{(n_{Hill})}] \quad (4)$$

where k_{max} is the maximal rate constant, $K_{D,M^{2+}}$ is the apparent dissociation constant of divalent metal, and n_{Hill} is the apparent Hill coefficient for divalent metal binding to the ribozyme.

RESULTS

To better explore the structural biology of the hammerhead ribozyme, we sought to identify and characterize a crystal form that differed significantly from the previously described crystals of the ribozymes from *S. mansoni*[24,26] and satellite tobacco ringspot virus.[42] We selected RzB, an artificially evolved variant of the hammerhead ribozyme with an alternate tertiary contact between stems I and II.[41] Several variants were screened to identify RNAs that would readily crystallize, and the sequence used in this study is shown in Figure 1. To prevent cleavage of the substrate RNA strand during crystallization and data collection, C17 was replaced with a deoxynucleotide, a substitution that deletes the nucleophile. Crystallization screens were performed under relatively low monovalent salt conditions that would allow Mg^{2+} ions and other divalent metals to interact with the ribozyme. The structures described here have been determined at a resolution of 2.7−3.1 Å. Data collection and refinement statistics can be found in Table 1, and composite omit maps are shown in Supporting Information, Figure S1.

The RNA crystallizes as a domain-swapped dimer in which one strand from stem Ia forms intermolecular base pairs with a second molecule within the unit cell (Supporting Information, Figure S2). The two monomers are related by crystallographic symmetry. Although the RNA strands are swapped to form the dimer, a monomer model can be generated by switching the crossed over strands (Supporting Information, Figure S1). In spite of the intermolecular crystal contact, the tertiary contact between stem I and stem II appears to be intact (Supporting Information, Figure S3). Loop II forms a pocket in which an adenosine from stem I can dock. The U at position L2.1 and A at position L2.5 form a Hoogsteen base pair. The A at position L1.3 in stem I is extruded and stacks upon the Hoogsteen base pair from loop II and the Watson−Crick face of L1.3 hydrogen bonds to the minor groove face of the first G in loop II. Overall, the topology of the three guanosines in loop II resembles that of a GNRA tetraloop with a long-range tertiary interaction taking the place of the adenosine normally found at the last position of the tetraloop (Supporting Information, Figure S3).

The conformation of the active site of hammerhead ribozyme depends critically on the tertiary interaction between stem I and stem II. The active site of the RzB hammerhead ribozyme is strikingly similar to that observed in the *S. mansoni* hammerhead ribozyme and differs significantly from the structure of the minimal hammerhead ribozyme. This suggests that the active site structure observed in crystals of the RzB hammerhead ribozyme is native in spite of the base pairing formed across the molecules in the crystals (Figure 3). The structural similarities between the *S. mansoni* and RzB ribozymes remain in spite of the differences in sequence, in crystal contacts, and in crystallization conditions. We therefore used these crystals and this RNA sequence to explore the roles of divalent metal ions and individual nucleotides to hammerhead ribozyme catalysis.

The G12A Mutation Is Disruptive to Catalysis. We next investigated the proposed general base, G12. Mutation of the highly conserved G12 nucleotide to an adenosine severely reduced the k_{obs} of the reaction in 10 mM Mg^{2+} at pH 6.5 (Table 2). The rate constant for the reaction of the WT ribozyme was measured to be ∼1.4 min^{-1}. In contrast, the k_{obs} measured for G12A under similar conditions was ∼0.00011 min^{-1}, which represents about a 13 000-fold decrease in the reaction rate. Such a low reaction rate is consistent with previous studies showing the importance of G12 for the cleavage reaction.[23,42,47]

To confirm that the G12A mutation does not cause significant structural changes in the RzB ribozyme, we determined the crystal structure of the G12A mutant ribozyme (Figure 4). As previously observed, there are minimal structural differences between the WT ribozyme and G12A mutant.[42,47] The ribozyme was crystallized with a deoxynucleotide at C17, and therefore an exact measurement between the N1 of the purine at position 12 and the 2′-hydroxyl of C17 is impossible. The distance between C2′ of C17 and the N1 of A12 in the G12A crystal structures is 4.0 Å, while the equivalent distance is 4.2 Å for the N1 of G12 in the WT ribozyme. The distance of the proposed general acid, the 2′-OH of G8 to the 5′-O leaving group on U1.1, remains unchanged at 3.2 Å in both the G12A mutant and WT ribozymes. Thus, the A12 mutation does not appear to cause significant structural changes in the ground state conformation observed in the crystal structure.

It has been reported previously that the observed rate at which WT ribozyme cleaves increases log−linearly with respect to pH.[23,33] A similar pH−rate profile was obtained for the WT ribozyme in 5 mM Mg^{2+} (Figure 5). The observed rate constant is observed to be log−linear from pH 4.5 through ∼

DOI: 10.1021/acs.biochem.5b00824
Biochemistry 2015, 54, 6369−6381

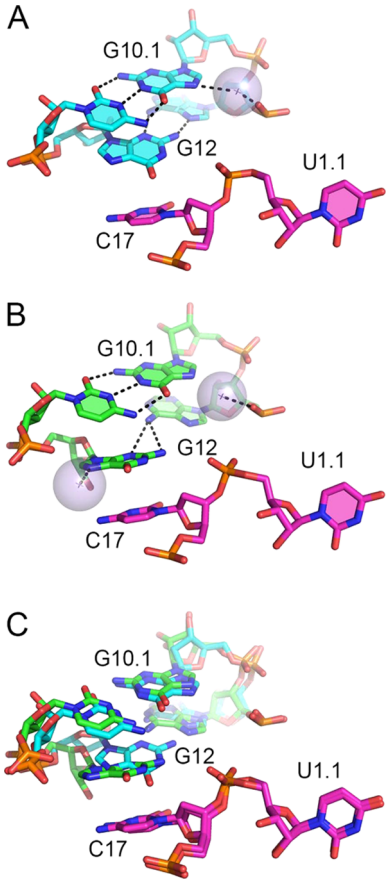

Figure 3. A pH-dependent conformational rearrangement of the active site. (A) At pH 5.0, G12 is observed to be involved in a sheared base pair with A9. A single Mn^{2+} ion is observed in the active site near G10.1. (B) At pH 8.0, G12 has changed position to stack upon C17. Two long, ~3.5 Å, potential hydrogen bonds link G12 and A9. Two Mn^{2+} ions are observed in the active site at pH 8.0. The first, near G10.1 as seen at pH 5.0. The second is observed at the Hoogsteen face of G12. (C) The structures of the RzB hammerhead ribozyme at pH 5.0 and 8.0 were superposed based on the position of the cleavage site dinucleotide (pink). Active site nucleotides are shown in cyan (pH 5.0) and green (pH 8.0). The largest difference in the two structures is the position of G12. Movement of G12 away from the scissile phosphate and the recruitment of a metal ion (shown in panel B) to G12 suggest that G12 may be deprotonated and negatively charged at pH 8.0.

Table 2. Observed Rate Constants for WT RzB Hammerhead Ribozyme and Its Mutants[a]

	k_{obs} (min^{-1})	k_{rel}[b]
WT	1.39 ± 0.04	NA
G12A	0.00011 ± 0.00003	0.00008
G10.1C/C11.1G	0.00132 ± 0.00008	0.001
G10.1A/C11.1U	0.078	0.06

[a]Reactions were performed at 37 °C under single turnover conditions in 5 mM Mg^{2+} and 50 mM MES pH 6.5. [b]k_{rel} represents the ratio of the observed rate constant to that of the WT RzB hammerhead ribozyme.

pH 8.0. Such a profile is consistent with a theoretical pH−rate profile that would arise from a general base having a pK_a of ~8 (N1 of G12), and thus is largely consistent with the mechanism proposed by Scott.[24] The change in slope at pH 8.0 suggests that the N1 of G12 may have a pK_a that is lowered toward

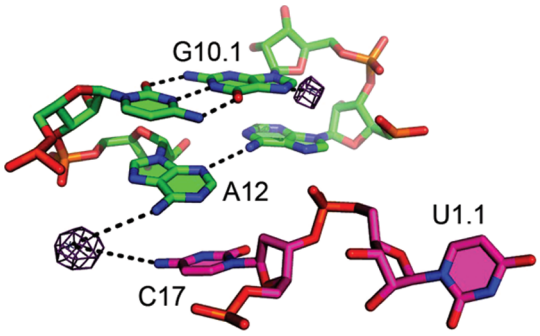

Figure 4. Active site of the G12A mutant hammerhead ribozyme. The structure of the G12A mutant ribozyme is very similar to that of the WT ribozyme. Due to the loss of the N2 exocyclic amine at position A12 is displaced slightly from the position occupied by G12 in the WT ribozyme. There is a 3.1 Å hydrogen bond between the N3 of A12 and the N6 of A9. Crystals of the G12A mutant ribozyme were soaked in 10 mM $Zn(O_2CCH_3)_2$ prior to freezing, and anomalous diffraction data were collected using X-rays at a wavelength of 1.181 Å. An anomalous difference density map, shown here contoured at 4σ, was used to indentify Zn^{2+} binding sites within the ribozyme. A clear peak for Zn^{2+} is observed near A12. The distance between the N6 of A12 and the Zn^{2+} ion is 4.5 Å, and the distance between the N4 of C17 and the Zn^{2+} ion is 5.1 Å. In addition, a Zn^{2+} ion occupies the divalent ion binding pocket near G10.1.

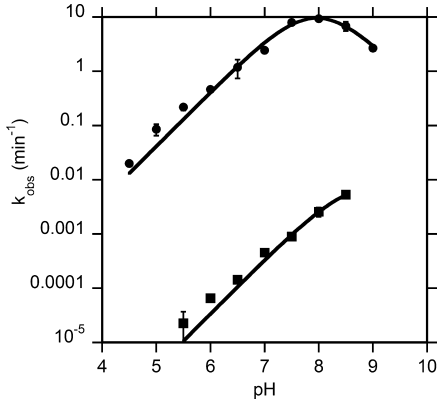

Figure 5. pH−rate profile of WT hammerhead ribozyme (circles) is compared to pH−rate profile of G12A (squares). Single turnover reactions were performed in 50 mM appropriate buffer. WT ribozyme reactions were conducted using a 5 mM Mg^{2+} concentration, and G12A mutant ribozyme reactions were performed at 50 mM Mg^{2+}. Data were fit to eq 3 or to a line as appropriate. Error bars represent standard deviations from at least three replicates.

neutrality in the context of the folded hammerhead ribozyme as suggested previously.[48] Above pH 8.5, the rate constant decreases, and it is not clear if this is due to deprotonation of a general acid, such as the 2′-OH of G8 or a water molecule, being deprotonated or if this is due to denaturation of the RNA.

In the G12A mutant, however, the pH−rate profile would be expected to be significantly different than that observed for the wild type ribozyme. Adenosine in solution has a pK_a of ~3.5. A general base with that pK_a and a general acid with a pK_a ≈ 13 would be expected to give rise to a pH−rate profile that is flat in the measurable pH range (Supporting Information, Figure S5). We characterized the pH−rate profile of the G12A mutant using 50 mM Mg^{2+} where the reaction is faster, allowing more accurate measurements to be made (Figure 5). As with the WT ribozyme, the pH−rate profile of the G12A mutant is log−

DOI: 10.1021/acs.biochem.5b00824
Biochemistry 2015, 54, 6369−6381

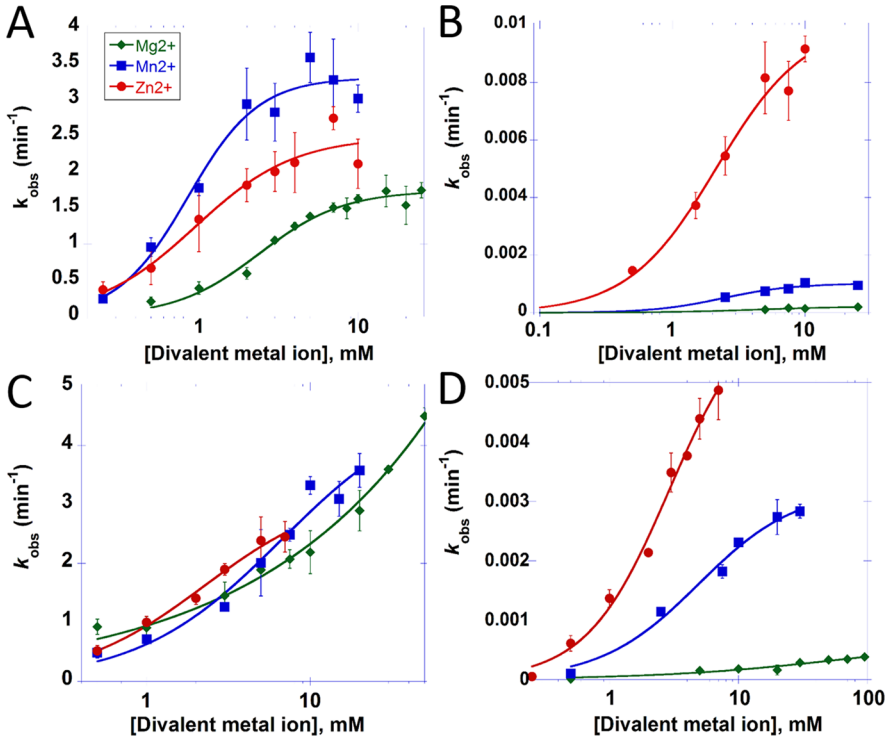

Figure 6. G12A mutant shows a metal ion specificity switch. Single turnover reactions were performed in Mg^{2+} (green ◊), Mn^{2+} (blue □), or Zn^{2+} (red ○). Reactions contained 2 μM ribozyme, 50 nM fluorescently labeled substrate, and 50 mM MES pH 6.5. The reactions were performed using RzB hammerhead ribozyme (A) or the G12A mutant (B). Data from these graphs were fit to eq 4, and the resulting parameters are given in Table 3. Measurements at higher Zn^{2+} concentrations were not possible due to the loss of Zn^{2+} solubility. Error bars represent standard deviation from three replicates. The *S. mansoni* hammerhead ribozyme was characterized under the same conditions in panels (C) (WT) and (D) (G12A).

linear; however, a change in the slope at high pH is not observed with this mutant (Figure 5). As the G12A mutant replaces a potential general base with a pK_a of ∼9 with a potential general base with a pK_a of around 4, these data suggest either that the pH−rate profile of the hammerhead ribozyme does not reflect the protonation state of G12 or that the mechanism of the G12A mutant must be revisited.

A pH-Dependent Conformational Switch in the Hammerhead Ribozyme Active Site. The hammerhead ribozyme exhibits maximal activity at high pH. We therefore compared crystal structures of the hammerhead ribozyme at pH 5.0 and pH 8.0 (Figure 3). The WT ribozyme exhibits maximal activity at pH 8.0 with the observed rate constant about 3 orders of magnitude higher in pH 8.0 than in pH 5.0. In both structures, $MnCl_2$ was included in the soaking buffer to allow unambiguous identification of divalent metal binding sites using anomalous diffraction.

A significant rearrangement of the active site of the hammerhead ribozyme is observed at pH 8.0. The observed changes in conformation are centered around G12 (Figure 3C). At pH 5.0, G12 makes a sheared base pair with A9 with two hydrogen bonds formed between the two bases. When the pH is shifted to pH 8.0, this base pair is disrupted and G12 shifts 2−3 Å away from A9 to stack upon C17. The only other significant shift is at nucleotide A9, which shifts in the same direction but only ∼1−1.5 Å. In these crystal structures, we are missing the 2′-OH nucleophile, and therefore it is difficult to determine how the distance from G12 to the nucleophile changes. However, the distance from the N1 of G12 to the phosphorus atom of the scissile phosphate can be readily measured. At pH 5.0, this distance is 5.4 Å, and at pH 8.0, this distance is 5.9 Å.

The locations of Mn^{2+} ions can be unambiguously identified in these structures through anomalous scattering experiments. At both pH 5.0 and pH 8.0, an Mn^{2+} ion is observed near G10.1 as previously described.[37] An additional Mn^{2+} ion is observed to bind near the Hoogsteen face of G12, but only at pH 8.0 (Figure 3 and Supporting Information, Figure S6). The position of this Mn^{2+} ion suggests that the coordination to N7 of G12 is direct, while coordinate of O6 of the metal ion of G12 is outer sphere and mediated by a metal-bound water molecule. If a Mg^{2+} ion were to bind at this site, the ligands would be expected to be slightly different as Mg^{2+} does not usually coordinate directly to the N7 nitrogen.

It is impossible to tell from a static crystal structure if the observed change in conformation is due to a change in the ionization state of a functional group on the ribozyme or which functional group is ionizing. However, there is striking change in conformation of G12 and a small, but significant movement away from the negatively charged scissile phosphate. In addition, a positively charged metal ion is only observed to associate with G12 at pH 8.0. Both of these observations suggest that G12 may be deprotonated and negatively charged at pH 8.0, consistent with the inflection point observed in the pH−rate profile. Curiously, at high pH, G12 is in a position similar to that of A12 in the G12A mutant. If G12 is, in fact, deprotonated at pH 8.0, this similarity may reflect the conversion of the hydrogen bond donor at N1 of G12 into a hydrogen bond acceptor.

The G12A Mutation Exhibits a Metal Ion Specificity Switch. Several studies have shown that the divalent metals

DOI: 10.1021/acs.biochem.5b00824
Biochemistry 2015, 54, 6369−6381

Table 3. Kinetic Parameters for Hammerhead Ribozyme Cleavage Reactions in Various Divalent Metal Ions[a]

	WT			G12A		
	Zn^{2+}	Mn^{2+}	Mg^{2+}	Zn^{2+}	Mn^{2+}	Mg^{2+}
RzB						
k_{max} (min^{-1})	1.7 ± 0.1	3.3 ± 0.2	2.5 ± 0.3	0.010 ± 0.001	0.0010 ± 0.0001	0.0002 ± 0.0001
K_D (mM)	2.4 ± 0.2	0.9 ± 0.1	1.0 ± 0.2	2.1 ± 0.6	2.4 ± 0.5	4.0 ± 3
n_{Hill}	1.7 ± 0.3	2.0 ± 0.5	1.4 ± 0.4	1.3 ± 0.3	1.7 ± 0.8	1.3 ± 3
S. mansoni						
k_{max} (min^{-1})	3.2 ± 0.5	5 ± 1		0.007 ± 0.001	0.0023 ± 0.0003	0.0005 ± 0.0001
K_D (mM)	2.3 ± 0.8	7 ± 4		2.9 ± 0.9	2.5 ± 1.0	19 ± 9
n_{Hill}	1.1 ± 0.2	1.0 ± 0.3		1.4 ± 0.3	2.2 ± 2	0.7 ± 0.2

[a]Reactions were performed in 50 mM MES pH 6.5 and various concentrations of the indicated divalent metal ion.

influence the observed rate constants in tertiary-stabilized hammerhead ribozyme.[33,34] In an attempt to understand how divalent metals impact the reaction, metal ion titration studies were performed using both WT and G12A mutant ribozymes. For this study, we focused on the response of the hammerhead ribozyme to Mg^{2+}, Mn^{2+}, and Zn^{2+} ions. The pH was kept low (6.5) to avoid complications arising from lower solubility of divalent metals at higher pH conditions. For the wild-type RzB ribozyme, the k_{obs} values only show minor differences between Mn^{2+}, Mg^{2+}, or Zn^{2+} (Figure 6). Reactions in Zn^{2+} and Mn^{2+} appear slightly faster when compared to Mg^{2+} as previously observed;[33] however the observed k_{max} values in the different metal ions are within 2-fold of each other (Table 3). Likewise, the reactions in the various metal ions exhibit only small differences between the apparent K_D's and Hill coefficients.

In contrast, the G12A mutant of RzB ribozyme shows a very different preference for divalent metals than the wild-type ribozyme. The observed rate constant was significantly higher in Zn^{2+} as compared to Mn^{2+} or Mg^{2+} (Figure 6B). k_{max} of the RzB G12A mutant in the presence of Zn^{2+} was ∼0.10 min^{-1}, which is 10-fold higher than that observed in Mn^{2+} and about 50-fold higher than that observed in Mg^{2+}. The trends in apparent dissociation constants and Hill coefficients remain similar to those observed in the wild-type RzB ribozyme. In contrast to the 13 000-fold difference in reactivity between the WT and G12A mutant ribozymes in Mg^{2+} ion, there is only a 170-fold difference in k_{max} between the WT and G12A mutant ribozymes in Zn^{2+} ion (Table 3).

Metal specificity switches can result from binding of metal ions at locations distant from the active site. We therefore repeated these experiments using the *S. mansoni* hammerhead ribozyme. This ribozyme has different sequences in the peripheral helices, but the core nucleotides in the active site are invariant. It was not possible to saturate the reaction of the WT *S. mansoni* hammerhead ribozyme with Mg^{2+} precluding an accurate description of the kinetic parameters for the reaction in this ion. The observed rate constants in all three metal ions, however, are similar (Figure 6, Table 3). We then examined the metal ion dependence of the *S. mansoni* G12A mutant. This ribozyme displays the same preference for the divalent metals as the RzB G12A mutant ribozyme (Figure 6, Table 3). Zn^{2+} significantly enhances the reactivity over that observed in Mn^{2+} or Mg^{2+}. As with the WT *S. mansoni* ribozyme, saturation was not observed in the Mg^{2+}-containing reactions. These experiments demonstrate that replacing G12 with an adenosine switches the divalent metal binding preference in at least two hammerhead ribozyme sequences. As the metal ion specificity switch is observed in different ribozymes with different peripheral elements, the switch in divalent metal specificity is likely a conserved property of the catalytic core nucleotides in the active site of the G12A mutant.

A Zn^{2+} Ion Binding Pocket at A12. To characterize the metal ion binding properties of the G12A mutant ribozyme, we soaked crystals of this ribozyme in stabilization buffer containing Zn^{2+} and collected anomalous diffraction data from the Zn^{2+} soaked crystals. A >5σ peak is observed near A12 in the Zn^{2+} anomalous density map (Figure 4). Potential ligands to this Zn^{2+} ion are the exocyclic amine of A12 (4.5 Å distant), the pro-S_P oxygen of U16.1 (4.1 Å distant), and the exocyclic amino of C17 (5.1 Å distant). These distances are consistent with outer sphere interactions between the ligands from the RNA and the water molecules bound to the hydrated Zn^{2+} ion. Mn^{2+} is observed at the same site in an anomalous difference map obtained using an Mn^{2+} soaked crystal. However, the peak from the Mn^{2+} ion is only ∼3.5σ in height, consistent with lower occupancy and weaker rescue of the G12A mutant ribozyme with Mn^{2+}.

There Is a Divalent Metal Ion Binding Pocket at G10.1. A divalent metal ion has been previously observed at the G10.1−C11 base pair in the crystal structure of the *S. mansoni* hammerhead ribozyme. There is significant evidence to suggest that this metal ion participates in catalysis and interacts with the scissile phosphate during the cleavage reaction.[28,29] In the RzB ribozyme, we are also able to observe electron density at the Hoogsteen face of G10.1 that appears to be a Mg^{2+} ion. To confirm metal ion binding at this position, we soaked crystals in Mn^{2+} and calculated anomalous difference electron density maps. At pH 5.0 Mn^{2+} ion at G10.1 gives rise to a > 5σ peak (Figure 3). As has been observed previously with the *S. mansoni* hammerhead ribozyme,[37] this ion is 4−5 Å distant from the scissile phosphate in the ground state crystal structure.

To characterize the role of the metal ion bound near G10.1, double mutants were generated that preserved the base-pairing potential of nucelotides 11.1 and 10. The G10.1C−C11G double mutant swaps the positions of the purine and the pyrimidine in the base pair. Thus, the N7 on guanosine is moved to the opposing strand of RNA, and the exocyclic amine of the cytosine occupies the major groove near the metal binding site. Secondary structure predictions suggest that this double mutant retains the ability to fold into the wild-type secondary structure. The activity of this mutant is 1050-fold lower relative to that of the wild-type ribozyme (Table 2). The G10.1A−C11U double mutant retains the purine and the N7 at the 10.1 position but replaces the keto group of the guanosine with the exocyclic amine of an adenosine. This double mutant is also predicted to retain the secondary structure of the wild-type ribozyme. The A10.1−U11 double mutant is only 18-fold less active than the WT ribozyme. These results are consistent

DOI: 10.1021/acs.biochem.5b00824
Biochemistry 2015, 54, 6369−6381

with previous studies of the minimal hammerhead ribozyme that probed base pairing between G10.1 and C11 and the role of the N7 of G10.1.[49]

The mutagenesis experiments suggest that the metal ion binding site at the G10.1−C11 base pair is important for catalysis, in spite of being 4−5 Å distant from the cleavage site dinucleotide. Loss of the N7 on the purine is expected to be highly disruptive to metal ion binding, while replacement of the keto oxygen on the guanosine with the exocyclic amino group of adenosine is expected to be modestly disruptive.

DISCUSSION

The hammerhead ribozyme has been extensively characterized since it was first discovered in 1987. Early studies focused on a minimal ribozyme design containing only the core nucleotides in the active site and three small stems. This molecule was systematically studied using a variety of single atom substitutions and unnatural nucleotides.[50] The crystal structure of the minimal hammerhead ribozyme was also the very first ribozyme to be characterized by X-ray crystallography.[51,52] Surprisingly at the time, the crystal structure of the minimal hammerhead ribozyme was not supported by the extensive biochemical data (reviewed in ref 50), suggesting that the structure was not in a catalytically active conformation. Eventually, a tertiary contact between stem I and stem II of the hammerhead ribozyme was discovered to exist in naturally occurring hammerhead ribozymes. When the hammerhead ribozyme is extended to include this tertiary contact, the reactivity of the ribozyme is greatly increased.[41,53−55] As predicted by the biochemical data, this tertiary contact is necessary to reorganize the conformation of the active site, and the crystal structure of the tertiary-contact stabilized ribozyme revealed a distinctly different conformation in the active site. The structure of the active site in the extended hammerhead is in agreement with most of the available biochemical data.[56,57] Crystal structures, however, only reveal the structure of a trapped ground state, and evidence is accumulating that suggests the active site of the hammerhead must further rearrange prior to catalysis or during the reaction pathway.

The Curious Case of G12. In all the crystal structures of the extended hammerhead, G12 is pointed toward the position that would be occupied by 2′-hydroxyl of U16.1, the nucleophile in the cleavage reaction. G12 has been proposed to serve as the general base, capable of accepting a proton from the nucleophile when G12 is in its deprotonated, negatively charged, state. Guanosine at position 12 is completely conserved in all known hammerhead ribozymes, and substitution with adenosine or unnatural purine analogues, including 2,6-diaminopurine, inosine, and 2-aminopurine, is more detrimental to catalysis than would be predicted based on the position of G12 within the active site and its function as a general base.[23,47]

G12 and A9 form a sheared base pair, and there is a hydrogen bond between the exocyclic amine of G12 and the N7 of A9. Surprisingly, substitution of G12 with an inosine, which lacks only the exocyclic amine, is severely disruptive to catalysis.[47,58] Inosine has a pK_a similar to that of guanosine (9.6 for guanosine vs 8.7 for inosine), and an inosine at position 12 would be expected to largely retain function. The nucleobases 2-aminopurine or 2,6-diaminopurine retain the exocyclic amine at position 2, but either lacks a functional group at position 6 or substitutes an exocyclic amine for the keto oxygen of guanine. Like adenosine, 2-aminopurine and 2,6-diaminopurine nucleobases severely reduce cleavage activity when introduced at position 12. Comparing the activity for all of these nucleobase substitutions suggests that maximal activity requires both an exocyclic amine at position 2 and either a keto oxygen or an exocyclic amine at position 6. This requirement is not supported by the crystal structures as the keto oxygen of G12 points toward solvent and is not engaged in any hydrogen bonds or direct metal ion interactions (Figure 3).

More curiously, all of these purine analogues retain the ability to perform proton transfer reactions and would be expected to support function in the hammerhead ribozyme cleavage reaction. The pK_a's of the purines used in these studies ranges from ∼4 to ∼9. Yet, the pH−rate profile for ribozymes with purine substitutions at position 12 are all very similar to a log linear profile from ∼ pH 4 to ∼ pH 8.5. If G12 were involved in a proton transfer reaction, the activity of the ribozyme would be expected to depend on the protonation state of G12 or the protonation state of the purine introduced at position 12. This is clearly not evident in the pH−rate profile.[23] This suggests either that the pH−rate profile does not reflect the protonation state of G12 or that the path to the cleavage reaction is more complex than expected based on the ground state crystal structure. Thus, G12 likely plays key roles in organization of the active site that have not yet been fully elucidated by the structures observed in the available crystals.

G12 Positions an Active Site Metal Ion. Here, we present data that suggest that the purine at position 12 plays critical roles in positioning an active site metal ion. As observed in previous studies, the activity of the G12A mutant ribozyme is over 4 orders of magnitude slower than the WT ribozyme in the presence of Mg^{2+}.[47] However, the maximal rate of the G12A ribozyme is only 2 orders of magnitude slower in the presence of the Zn^{2+} ion (Figure 4, Table 3). The interaction between A12 in the mutant ribozyme and the rescuing Zn^{2+} ion could be direct, or it could result from a long-range effect from Zn^{2+} binding elsewhere in the ribozyme. The Zn^{2+} rescue of the G12A mutant is not dependent on the identity of the hammerhead ribozyme as it is observed both in the RzB ribozyme and in the *S. mansoni* ribozyme. Thus, the rescuing Zn^{2+} likely binds to an active site nucleotide present in the catalytic core common to both ribozymes. In addition, we are able to observe a Zn^{2+} ion interacting with the Hoogsteen face of A12 in the mutant ribozyme (Figure 5). Both monovalent and divalent ions have been observed to interact with the Hoogsteen face of G12 in crystal structures described here and elsewhere.[26,37]

What role does the metal ion at the Hoogsteen face of position 12 play? One possibility is that this metal ion serves solely to lower the pK_a of G12 in the WT ribozyme through electrostatic effects. However, the Zn^{2+} rescue of the G12A mutant argues against this. Just as metal ion binding at the Hoogsteen face of G12 could shift the pK_a of G12 down toward neutrality, metal ion binding at A12 in the mutant ribozyme would be expected to shift the pK_a of A12 down. But this shift would push the pK_a of A12 below ∼4 and away from neutrality. While this positively charged metal ion could stabilize the negative charge at the N1 in the deprotonated state of G12, it should destabilize protonation of A12 due to juxtaposition of multiple positive charges (Figure 7). Thus, binding of metal ion at the Hoogsteen face would be expected to disfavor proton transfer if A12 were serving as the general base in this mutant, and the only role for Zn^{2+} were to lower the pK_a of the purine nucleobase (Figure 7). In contrast to the inhibition expected in

DOI: 10.1021/acs.biochem.5b00824
Biochemistry 2015, 54, 6369−6381

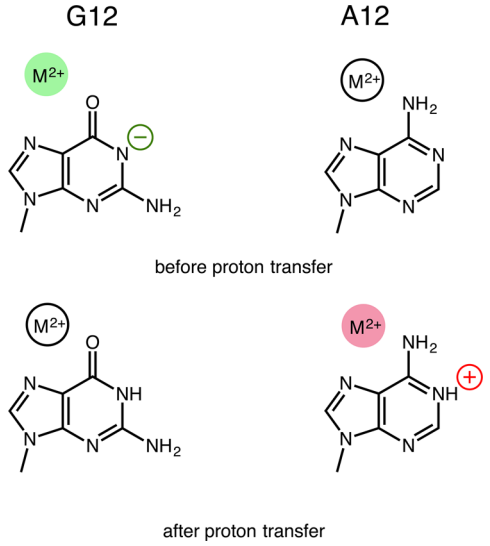

Figure 7. Metal ion activation of G12. Coordination of a divalent metal ion to G12 is predicted to lower the pK_a of the nucleobase from ~9 toward neutrality because the positively charged metal ion can stabilize the negative charge on the guanine base. In contrast, metal ion binding to adenine is predicted to shift the pK_a of the adenine nucleobase away from neutrality as the metal ion would destabilize the positively charged, protonated form of the nucleobase.

this scenerio, however, we observe that Zn^{2+} rescues the G12A mutant to within 2 orders of magnitude of the WT ribozyme. This suggests that the rescuing Zn^{2+} enhances the reactivity of the G12A mutant through a different mechanism.

The location of the rescuing metal ion observed in Zn^{2+} anomalous difference maps of the G12A ribozyme is also problematic. This Zn^{2+} has three potential ligands that are atoms within the covalent structure of the ribozyme. However, all of these atoms are >4.5 Å distant from the metal ion, suggesting the metal ion only interacts with the RNA through its water shell (Figure 4). Most metal ion specificity switches result from metal ions coordinating directly to atoms within the covalent structure of RNA. In addition, the metal ion is at the periphery of the RNA, distant from most of the active site and the cleavage site (Figure 4). Combined, the specificity switch and the location of the Zn^{2+} ion near A12 suggest that the hammerhead ribozyme undergoes a conformational change prior to or during the cleavage reaction. This proposed conformational change could serve to bring A12 into direct contact with the Zn^{2+} ion and give rise to the observed metal specificity switch.

Zn^{2+} Could Induce Tautomerization of A12. Zn^{2+} ions, while commonly found at the Hoogsteen face of guanosine nucleotides, are not observed to interact with adenosine nucleotides. The only difference between the Hoogsteen face of G and the Hoogsteen face of A is that the keto group at the six position of guanine is replaced with the exocyclic amine at the six position of adenine. Metal specificity switches typically result from a direct contact between a metal ion and the ligand being probed. The observed metal specificity switch would therefore suggest that the Zn^{2+} ion at the Hoogsteen face of A12 becomes directly coordinated to the N6 of A12 in the G12A mutant. Chemically, this is problematic because aromatic exocyclic amine groups are not particularly good metal ligands for Zn^{2+} (Figure 8). In addition, as previously discussed, a direct interaction between Zn^{2+} and A12 is expected to lower

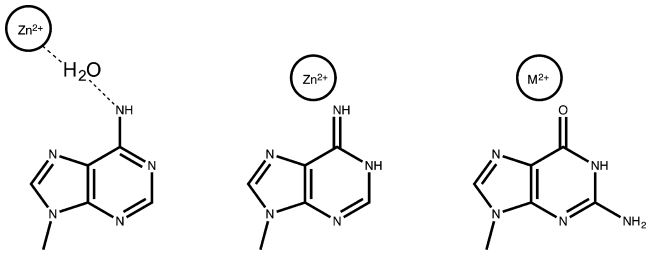

Figure 8. A conformational change is needed to stabilize the rare imino tautomeric form of A12. In the crystal (left), a Zn^{2+} ion is observed to coordinate the N6 of A12 through its water ligand. Divalent metal ions are observed to stabilize tautomeric forms of adenine; however, this involves direct coordination of the metal ion to the nucleobase.[62] Zn^{2+} rescue of the G12A mutant suggests that the Zn^{2+} ion could become directly coordinated to the N6 of A12, and the pH−rate profile of the G12A mutant is consistent with a model in which the reactive species is the rare imino tautomer (middle). In the WT ribozyme (right), a Mg^{2+} likely similarly coordinates to G12 to help lower the pK_a of G12 and organize the active site for catalysis.

the pK_a and impair, not improve, the ability of A12 to serve as a general base (Figure 7).

We propose a mechanism in which A12 tautomerizes during the cleavage reaction of the hammerhead ribozyme (Figure 8). Nucleobases have the ability to adopt tautomeric structures, especially when constrained in the context of protein or RNA active sites. Xanthine, a nucleobase not typically found in RNA, is observed to be in the rare tautomeric species when bound in the binding pocket of the purine riboswitch.[59] Rare tautomers of naturally occurring DNA nucleobases also appear to be trapped within the active site of polymerases.[60,61]

The imino-N1H tautomeric species of adenosine has chemical properties that could explain how the N6 of A12 could directly interact with the Zn^{2+} ion, and why the pH−rate profile of the G12A mutant differs so little from that of the WT ribozyme. If A12 adopted the imino-N1H tautomeric form in the context of the hammerhead ribozyme active site, N6 would become more electron-rich and therefore a better inner-sphere ligand to Zn^{2+}. Computational studies predict that interactions between divalent metal ions are strengthened in the rare, imino-NH1 species of adenine and, likewise, that the rare tautomeric species would be stabilized by the presence of the metal ion.[62] Thus, formation of the rare tautomer of adenine and stabilization of the same by Zn^{2+} coordinate could explain the observed metal specificity switch. This mechanism would predict that a Mg^{2+} ion is bound at a similar position to G12 in the WT ribozyme, leading to reduction in the pK_a and activation of the general base.

Tautomerization of A12 in the G12A mutation could also explain the pH−rate profile of the G12A mutant (Figure 5). If the dominant, amino, tautomer of A is functioning in the reaction, we would expect to see a different pH−rate profile in the WT and G12A mutant ribozyme reactions as the pK_a's of A and G differ significantly. However, the imino-N1H form of adenosine resembles guanosine in that N1 is protonated in its neutral form and the pK_a of this species would be predicted to be closer to that of guanine than that of adenine. If the minor, imino, tautomer of adenosine were to serve as a general base, the pH−rate profile for the G12A mutant ribozyme would therefore be expected to have the same overall shape as the WT ribozyme, as we observe. In addition, the same driving forces that facilitate deprotonation of the N1 of guanosine could facilitate deprotonation of the imino-N1 tautomeric form of

DOI: 10.1021/acs.biochem.5b00824
Biochemistry 2015, 54, 6369−6381

A12. Such a mechanism would help to explain the increased reactivity of 2,6-diaminopurine relative to 2-aminopurine at position 12 as a metal ion can interact with and stabilize the N6 imino-N1H tautomer of 2,6-diaminopurine nucleobase, but not the 2′-aminopurine nucleobase. We would predict that if G12 were replaced with a 2,6-diaminopurine, Zn^{2+} could further enhance the cleavage activity as this nucleobase possesses the N2 exocyclic amine lacking from adenine.

Active Site Rearrangements during the Hammerhead Ribozyme Cleavage Reaction. There are significant indications presented here and elsewhere[31,38,63] that the ground-state structure of the hammerhead ribozyme observed in crystals must undergo a significant conformational change prior to or during the cleavage reaction. We are able to observe a striking change in the position of G12 at high pH where the hammerhead ribozyme is the most active. We cannot determine if the change in the conformation of the ribozyme is due to deprotonation of G12. However, the change in position of G12 is consistent with deprotonation of the nucleobase as G12 is observed to move away from the scissile phosphate, yet remain in position to deprotonate the nucleophile. Such a change in conformation in the active site has not previously been observed.

The location of the two active site metal ions in the available crystal structures suggests that significant additional conformational changes are likely needed to occur prior to or during the cleavage reaction. The metal ion near G12 appears to be critical for ribozyme function, yet at maximum, this ion has a single inner-sphere ligand to the ribozyme and is located at the periphery of the active site. The metal ion at G10.1 is also distal to the active site, yet significant evidence exists that it contacts the scissile phosphate prior to the cleavage reaction, and this has not been observed in any crystal structure. Wang et al. elegantly linked Cd^{2+} rescue of phosphorothioate-substitutions at A9 and the pro-R_P oxygen of the scissile phosphate to the N7 of G10.1 in the context of a minimal hammerhead ribozyme that lacks the tertiary contact between stems I and II.[28] These data suggest that the metal binding pocket near G10.1 must contract and bring the metal ion into proximity of the scissile phosphate. Ward et al. demonstrated that this metal ion interacts with the pro-R_P oxygen of the scissile phosphate in the ground state of the *S. mansoni* ribozyme. We are unable to observe metal binding at this position in any of the anomalous diffraction experiments described here. These data suggest that all of the crystal structures, including those presented here, represent an open structure that must subtly rearrange during the cleavage reaction.

CONCLUSIONS

Over 25 years after the discovery of the hammerhead ribozyme, we still do not fully understand how the hammerhead ribozyme performs its cleavage reaction. Most of the known small nucleolytic ribozymes appear to be largely preordered for catalysis. The hammerhead, however, seems to predominantly exist in an open and precatalytic state, and its cleavage mechanism appears to involve significant molecular motions. In addition, there are at least two distinct divalent metal ions involved in the cleavage reaction. One, near G10.1, is well characterized and predicted biochemically to interact directly with the cleavage site and likely participates in the cleavage reaction. The second, observed here to be near G12, is predicted to be important for organization of the active site as it proceeds through the cleavage reaction and likely tunes the pK_a of G12.

Our studies of the G12A mutant suggest that rare nucleobase tautomers could potentially play key roles in ribozyme reaction mechanisms. While we observe this phenomenon in a mutant ribozyme, native, wild-type ribozymes could also use this mechanism. Tautomeric species may also be key intermediates in and facilitate nucleobase protonation/deprotonation reactions in the nucleolytic ribozymes.[64] Interpretation of pH-dependence is often complicated due to the principle of kinetic equivalence, in which different reaction mechanisms can give rise to the same pH−rate profile. Kinetic equivalence makes it difficult to unambiguously identify the general acid and general base in enzymatic reactions. Tautomerization of nucleobases has the potential to add further complexity to such interpretation as seen here, where mutations and substitutions of the general base do not result in predictable changes in the pH−rate profile of the hammerhead ribozyme. Many of the small nucleolytic ribozymes, including the hairpin, glmS, VS, and twister ribozymes, employ conserved guanosine nucleotides that are well positioned to serve as proton donors and acceptors.[65] Formation of tautomeric species, and the accompanying changes in pK_a, have the potential to complicate analysis of these ribozyme reactions. Thus, we still have much to learn about the mechanisms by which ribozymes can catalyze chemical reactions under biological conditions.

ASSOCIATED CONTENT

Supporting Information

The Supporting Information is available free of charge on the ACS Publications website at DOI: 10.1021/acs.biochem.5b00824.

Composite $2F_o - F_c$ omit maps contoured at 1.2σ (Figure S1), crystal contacts involving intermolecular base pairs (Figure S2), tertiary contact between stem I and loop 2 (Figure S3), sample kinetics gel (Figure S4), and simulated pH−rate profiles of WT RzB and G12A RzB (Figure S5) (PDF)

AUTHOR INFORMATION

Corresponding Author

*Telephone: (765) 496-6165; e-mail: barbgolden@purdue.edu.

Author Contributions

#A.M. and J.C. contributed equally.

Funding

This project was supported by National Institutes of Health Grant R01 GM095923 and S10 OD012041, the Purdue University Department of Biochemistry, the Markey Center for Structural Biology, and the Purdue University Center for Cancer Research. This research used resources of the Advanced Photon Source (a U.S. Department of Energy (DOE) Office of Science User Facility operated for the DOE Office of Science by Argonne National Laboratory under Contract No. DE-AC02-06CH11357), the NE-CAT beamlines [funded by NIH (P41 GM103403)], the Pilatus 6M detector on 24-ID-C beamline [funded by a NIH-ORIP HEI grant (S10 RR029205)] and the LS-CAT Sector 21 beamlines [supported by the Michigan Economic Development Corporation and the Michigan Technology Tri-Corridor (Grant 085P1000817)].

Notes

The authors declare no competing financial interest.

DOI: 10.1021/acs.biochem.5b00824
Biochemistry 2015, 54, 6369−6381

■ ACKNOWLEDGMENTS

We are grateful to Victoria DeRose and Dan Herschlag for critical and insightful comments.

■ ABBREVIATIONS

EDTA, ethylenediaminetetraacetic acid; MPD, 1,6-methylpentanediol; PAGE, polyacrylamide gel electrophoresis; RzB, an artificial hammerhead ribozyme; WT, wild-type

■ REFERENCES

(1) Uhlenbeck, O. C. (1987) A small catalytic oligoribonucleotide. *Nature 328*, 596−600.
(2) de la Peña, M., and García-Robles, I. (2010) Ubiquitous presence of the hammerhead ribozyme motif along the tree of life. *RNA 16*, 1943−1950.
(3) Perreault, J., Weinberg, Z., Roth, A., Popescu, O., Chartrand, P., Ferbeyre, G., and Breaker, R. R. (2011) Identification of Hammerhead Ribozymes in All Domains of Life Reveals Novel Structural Variations. *PLoS Comput. Biol. 7*, e1002031.
(4) Seehafer, C., Kalweit, A., Steger, G., Gräf, S., and Hammann, C. (2011) From alpaca to zebrafish: Hammerhead ribozymes wherever you look. *RNA 17*, 21−26.
(5) Cervera, A., and De la Peña, M. (2014) Eukaryotic penelope-like retroelements encode hammerhead ribozyme motifs. *Mol. Biol. Evol. 31*, 2941−2947.
(6) Golden, B. L. (2011) Two distinct catalytic strategies in the hepatitis δ virus ribozyme cleavage reaction. *Biochemistry 50*, 9424−9433.
(7) Suga, H., Cowan, J. A., and Szostak, J. W. (1998) Unusual metal ion catalysis in an acyl-transferase ribozyme. *Biochemistry 37*, 10118−10125.
(8) DeYoung, M. B., Siwkowski, A., and Hampel, A. (1997) Determination of catalytic parameters for hairpin ribozymes. *Methods Mol. Biol. 74*, 209−220.
(9) Hampel, A., and Cowan, J. A. (1997) A unique mechanism for RNA catalysis: the role of metal cofactors in hairpin ribozyme cleavage. *Chem. Biol. 4*, 513−517.
(10) Nesbitt, S., Hegg, L. A., and Fedor, M. J. (1997) An unusual pH-independent and metal-ion-independent mechanism for hairpin ribozyme catalysis. *Chem. Biol. 4*, 619−630.
(11) Klawuhn, K., Jansen, J. A., Souchek, J., Soukup, G. A., and Soukup, J. K. (2010) Analysis of metal ion dependence in glmS ribozyme self-cleavage and coenzyme binding. *ChemBioChem 11*, 2567−2571.
(12) Brooks, K. M., and Hampel, K. J. (2011) Rapid steps in the glmS ribozyme catalytic pathway: cation and ligand requirements. *Biochemistry 50*, 2424−2433.
(13) Gong, B., Chen, J. H., Chase, E., Chadalavada, D. M., Yajima, R., Golden, B. L., Bevilacqua, P. C., and Carey, P. R. (2007) Direct measurement of a pK(a) near neutrality for the catalytic cytosine in the genomic HDV ribozyme using Raman crystallography. *J. Am. Chem. Soc. 129*, 13335−13342.
(14) Guo, M., Spitale, R. C., Volpini, R., Krucinska, J., Cristalli, G., Carey, P. R., and Wedekind, J. E. (2009) Direct Raman measurement of an elevated base pKa in the active site of a small ribozyme in a precatalytic conformation. *J. Am. Chem. Soc. 131*, 12908−12909.
(15) Gong, B., Klein, D. J., Ferré-D'Amaré, A. R., and Carey, P. R. (2011) The glmS ribozyme tunes the catalytically critical pK(a) of its coenzyme glucosamine-6-phosphate. *J. Am. Chem. Soc. 133*, 14188−14191.
(16) Liberman, J. A., Guo, M., Jenkins, J. L., Krucinska, J., Chen, Y., Carey, P. R., and Wedekind, J. E. (2012) A transition-state interaction shifts nucleobase ionization toward neutrality to facilitate small ribozyme catalysis. *J. Am. Chem. Soc. 134*, 16933−16936.
(17) Nakano, S., Proctor, D. J., and Bevilacqua, P. C. (2001) Mechanistic characterization of the HDV genomic ribozyme: assessing the catalytic and structural contributions of divalent metal ions within a multichannel reaction mechanism. *Biochemistry 40*, 12022−12038.
(18) Roychowdhury-Saha, M., and Burke, D. H. (2007) Distinct reaction pathway promoted by non-divalent-metal cations in a tertiary stabilized hammerhead ribozyme. *RNA 13*, 841−848.
(19) Cerrone-Szakal, A. L., Chadalavada, D. M., Golden, B. L., and Bevilacqua, P. C. (2008) Mechanistic characterization of the HDV genomic ribozyme: the cleavage site base pair plays a structural role in facilitating catalysis. *RNA 14*, 1746−1760.
(20) Chen, J. H., Yajima, R., Chadalavada, D. M., Chase, E., Bevilacqua, P. C., and Golden, B. L. (2010) A 1.9 A crystal structure of the HDV ribozyme precleavage suggests both Lewis acid and general acid mechanisms contribute to phosphodiester cleavage. *Biochemistry 49*, 6508−6518.
(21) Veeraraghavan, N., Ganguly, A., Chen, J. H., Bevilacqua, P. C., Hammes-Schiffer, S., and Golden, B. L. (2011) Metal binding motif in the active site of the HDV ribozyme binds divalent and monovalent ions. *Biochemistry 50*, 2672−2682.
(22) Chen, J., Ganguly, A., Miswan, Z., Hammes-Schiffer, S., Bevilacqua, P. C., and Golden, B. L. (2013) Identification of the catalytic Mg^{2+} ion in the hepatitis delta virus ribozyme. *Biochemistry 52*, 557−567.
(23) Han, J., and Burke, J. M. (2005) Model for general acid-base catalysis by the hammerhead ribozyme: pH-activity relationships of G8 and G12 variants at the putative active site. *Biochemistry 44*, 7864−7870.
(24) Martick, M., and Scott, W. G. (2006) Tertiary contacts distant from the active site prime a ribozyme for catalysis. *Cell 126*, 309−320.
(25) Lambert, D., Heckman, J. E., and Burke, J. M. (2006) Three conserved guanosines approach the reaction site in native and minimal hammerhead ribozymes. *Biochemistry 45*, 7140−7147.
(26) Anderson, M., Schultz, E. P., Martick, M., and Scott, W. G. (2013) Active-site monovalent cations revealed in a 1.55-Å-resolution hammerhead ribozyme structure. *J. Mol. Biol. 425*, 3790−3798.
(27) Bevilacqua, P. C. (2003) Mechanistic considerations for general acid-base catalysis by RNA: revisiting the mechanism of the hairpin ribozyme. *Biochemistry 42*, 2259−2265.
(28) Wang, S., Karbstein, K., Peracchi, A., Beigelman, L., and Herschlag, D. (1999) Identification of the hammerhead ribozyme metal ion binding site responsible for rescue of the deleterious effect of a cleavage site phosphorothioate. *Biochemistry 38*, 14363−14378.
(29) O'Rear, J. L., Wang, S., Feig, A. L., Beigelman, L., Uhlenbeck, O. C., and Herschlag, D. (2001) Comparison of the hammerhead cleavage reactions stimulated by monovalent and divalent cations. *RNA 7*, 537−545.
(30) Scott, E. C., and Uhlenbeck, O. C. (1999) A re-investigation of the thio effect at the hammerhead cleavage site. *Nucleic Acids Res. 27*, 479−484.
(31) Ward, W. L., and Derose, V. J. (2012) Ground-state coordination of a catalytic metal to the scissile phosphate of a tertiary-stabilized Hammerhead ribozyme. *RNA 18*, 16−23.
(32) Murray, J. B., Seyhan, A. A., Walter, N. G., Burke, J. M., and Scott, W. G. (1998) The hammerhead, hairpin and VS ribozymes are catalytically proficient in monovalent cations alone. *Chem. Biol. 5*, 587−595.
(33) Roychowdhury-Saha, M., and Burke, D. H. (2006) Extra-ordinary rates of transition metal ion-mediated ribozyme catalysis. *RNA 12*, 1846−1852.
(34) Boots, J. L., Canny, M. D., Azimi, E., and Pardi, A. (2008) Metal ion specificities for folding and cleavage activity in the Schistosoma hammerhead ribozyme. *RNA 14*, 2212−2222.
(35) Kisseleva, N., Khvorova, A., Westhof, E., and Schiemann, O. (2005) Binding of manganese(II) to a tertiary stabilized hammerhead ribozyme as studied by electron paramagnetic resonance spectroscopy. *RNA 11*, 1−6.
(36) Vogt, M., Lahiri, S., Hoogstraten, C. G., Britt, R. D., and DeRose, V. J. (2006) Coordination environment of a site-bound metal ion in the hammerhead ribozyme determined by 15N and 2H ESEEM spectroscopy. *J. Am. Chem. Soc. 128*, 16764−16770.

DOI: 10.1021/acs.biochem.5b00824
Biochemistry 2015, 54, 6369−6381

(37) Martick, M., Lee, T. S., York, D. M., and Scott, W. G. (2008) Solvent structure and hammerhead ribozyme catalysis. *Chem. Biol. 15*, 332−342.
(38) Lee, T. S., Silva López, C., Giambasu, G. M., Martick, M., Scott, W. G., and York, D. M. (2008) Role of Mg^{2+} in hammerhead ribozyme catalysis from molecular simulation. *J. Am. Chem. Soc. 130*, 3053−3064.
(39) Lee, T. S., Giambaşu, G. M., Sosa, C. P., Martick, M., Scott, W. G., and York, D. M. (2009) Threshold occupancy and specific cation binding modes in the hammerhead ribozyme active site are required for active conformation. *J. Mol. Biol. 388*, 195−206.
(40) Wong, K. Y., Lee, T. S., and York, D. M. (2011) Active participation of Mg ion in the reaction coordinate of RNA self-cleavage catalyzed by the hammerhead ribozyme. *J. Chem. Theory Comput. 7*, 1−3.
(41) Saksmerprome, V., Roychowdhury-Saha, M., Jayasena, S., Khvorova, A., and Burke, D. H. (2004) Artificial tertiary motifs stabilize trans-cleaving hammerhead ribozymes under conditions of submillimolar divalent ions and high temperatures. *RNA 10*, 1916−1924.
(42) Chi, Y. I., Martick, M., Lares, M., Kim, R., Scott, W. G., and Kim, S. H. (2008) Capturing hammerhead ribozyme structures in action by modulating general base catalysis. *PLoS Biol. 6*, e234.
(43) Golden, B. L. (2007) Preparation and crystallization of RNA, in *Macromolecular Crystallography Protocols* (Doublié, J. W. a. S., Ed.) pp 239−257, Humana Press, New York.
(44) Otwinowski, Z., and Minor, W. (1997) Processing of X-ray Diffraction Data Collected in Oscillation Mode, in *Methods in Enzymology* (Carter, C. W., and Sweet, R. M., Eds.) pp 307−326, Academic Press, New York.
(45) Adams, P. D., Afonine, P. V., Bunkóczi, G., Chen, V. B., Davis, I. W., Echols, N., Headd, J. J., Hung, L. W., Kapral, G. J., Grosse-Kunstleve, R. W., McCoy, A. J., Moriarty, N. W., Oeffner, R., Read, R. J., Richardson, D. C., Richardson, J. S., Terwilliger, T. C., and Zwart, P. H. (2010) PHENIX: a comprehensive Python-based system for macromolecular structure solution. *Acta Crystallogr., Sect. D: Biol. Crystallogr. 66*, 213−221.
(46) Emsley, P., Lohkamp, B., Scott, W. G., and Cowtan, K. (2010) Features and development of Coot. *Acta Crystallogr., Sect. D: Biol. Crystallogr. 66*, 486−501.
(47) Schultz, E. P., Vasquez, E. E., and Scott, W. G. (2014) Structural and catalytic effects of an invariant purine substitution in the hammerhead ribozyme: implications for the mechanism of acid-base catalysis. *Acta Crystallogr., Sect. D: Biol. Crystallogr. 70*, 2256−2263.
(48) Thomas, J. M., and Perrin, D. M. (2008) Probing general base catalysis in the hammerhead ribozyme. *J. Am. Chem. Soc. 130*, 15467−15475.
(49) Peracchi, A., Beigelman, L., Usman, N., and Herschlag, D. (1996) Rescue of abasic hammerhead ribozymes by exogenous addition of specific bases. *Proc. Natl. Acad. Sci. U. S. A. 93*, 11522−11527.
(50) Blount, K. F., and Uhlenbeck, O. C. (2005) The structure-function dilemma of the hammerhead ribozyme. *Annu. Rev. Biophys. Biomol. Struct. 34*, 415−440.
(51) Pley, H. W., Flaherty, K. M., and McKay, D. B. (1994) Three-dimensional structure of a hammerhead ribozyme. *Nature 372*, 68−74.
(52) Scott, W. G., Finch, J. T., and Klug, A. (1995) The crystal structure of an all-RNA hammerhead ribozyme: a proposed mechanism for RNA catalytic cleavage. *Cell 81*, 991−1002.
(53) De la Peña, M., Gago, S., and Flores, R. (2003) Peripheral regions of natural hammerhead ribozymes greatly increase their self-cleavage activity. *EMBO J. 22*, 5561−5570.
(54) Khvorova, A., Lescoute, A., Westhof, E., and Jayasena, S. D. (2003) Sequence elements outside the hammerhead ribozyme catalytic core enable intracellular activity. *Nat. Struct. Biol. 10*, 708−712.
(55) Canny, M. D., Jucker, F. M., Kellogg, E., Khvorova, A., Jayasena, S. D., and Pardi, A. (2004) Fast cleavage kinetics of a natural hammerhead ribozyme. *J. Am. Chem. Soc. 126*, 10848−10849.
(56) Nelson, J. A., and Uhlenbeck, O. C. (2006) When to believe what you see. *Mol. Cell 23*, 447−450.
(57) Nelson, J. A., and Uhlenbeck, O. C. (2008) Hammerhead redux: does the new structure fit the old biochemical data? *RNA 14*, 605−615.
(58) Burke, D. H., and Greathouse, S. T. (2005) Low-magnesium, trans-cleavage activity by type III, tertiary stabilized hammerhead ribozymes with stem 1 discontinuities. *BMC Biochem 6*, 14.
(59) Gilbert, S. D., Reyes, F. E., Edwards, A. L., and Batey, R. T. (2009) Adaptive ligand binding by the purine riboswitch in the recognition of guanine and adenine analogs. *Structure 17*, 857−868.
(60) Bebenek, K., Pedersen, L. C., and Kunkel, T. A. (2011) Replication infidelity via a mismatch with Watson-Crick geometry. *Proc. Natl. Acad. Sci. U. S. A. 108*, 1862−1867.
(61) Wang, W., Hellinga, H. W., and Beese, L. S. (2011) Structural evidence for the rare tautomer hypothesis of spontaneous mutagenesis. *Proc. Natl. Acad. Sci. U. S. A. 108*, 17644−17648.
(62) Ai, H., Chen, J., and Zhang, C. (2012) Amino-imino adenine tautomerism induced by the cooperative effect between metal ion and H2O/NH3. *J. Phys. Chem. B 116*, 13624−13636.
(63) Buskiewicz, I. A., and Burke, J. M. (2012) Folding of the hammerhead ribozyme: pyrrolo-cytosine fluorescence separates core folding from global folding and reveals a pH-dependent conformational change. *RNA 18*, 434−448.
(64) Singh, V., Fedeles, B. I., and Essigmann, J. M. (2015) Role of tautomerism in RNA biochemistry. *RNA 21*, 1−13.
(65) Ward, W. L., Plakos, K., and DeRose, V. J. (2014) Nucleic acid catalysis: metals, nucleobases, and other cofactors. *Chem. Rev. 114*, 4318−4342.
(66) Hertel, K. J., Pardi, A., Uhlenbeck, O. C., Koizumi, M., Ohtsuka, E., Uesugi, S., Cedergren, R., Eckstein, F., Gerlach, W. L., and Hodgson, R. (1992) Numbering system for the hammerhead. *Nucleic Acids Res. 20*, 3252.

DOI: 10.1021/acs.biochem.5b00824
Biochemistry 2015, 54, 6369−6381